

# Experimental Investigation of Thermal Performance of Three Configurations Evaporative Cooling Systems (ECS) Using Synthetic Grass Wet Media Materials

Sultan Alfraidi<sup>\*1</sup>, Abdelhakim Mesloub<sup>1</sup>, Mohammad Alshenaifi<sup>1</sup>, Emad Noaime<sup>1</sup>, Atef Ahriz<sup>2</sup>, R. Boukhanouf<sup>3</sup>

<sup>1</sup> Department of Architectural Engineering, Ha'il University, Ha'il 2440, Saudi Arabia

<sup>2</sup> Department of Architecture, Echahid Cheikh Larbi Tebessi University, Constantine Road, Tebessa 12000, Algeria.

<sup>3</sup> University of Nottingham, Department of Architecture and Built Environment, Nottingham, UK.

\*Corresponding Author: s.alfraidi@uoh.edu.sa

## Abstract

Space cooling of buildings using evaporative cooling is a passive strategy that can provide thermal comfort for occupants and conserve energy. In this paper, an innovative evaporative cooling wet media material in the form of synthetic grass fibre mat was introduced to evaluate experimentally its effectiveness in Direct Evaporative Cooling (DEC), Indirect Evaporative Cooling (IEC), and Dew point evaporative cooling (DPEC). A laboratory evaporative cooling module was constructed and tested using a fully instrumented test rig and was subject to environmentally controlled conditions of air temperature and relative humidity (RH) commensurate to those prevailing in hot and dry climates like the Middle East. The wet bulb effectiveness and cooling capacity of evaporative coolers equipped with the new wet media material were evaluated experimentally. The results show that these evaporative coolers performance correlate well with current technology. For instance, the ambient air temperature is reduced by as much as 12.9°C, 10.2°C, and 10.3°C for direct, indirect, and dew point modes, respectively. It was also shown that DEC achieved effectiveness 20% higher than indirect evaporative coolers. The work demonstrated that the new wet media can be a viable alternative to organic and non-organic counterparts.

**Keywords:** evaporative cooling; experiment; wet media; synthetic grass; hot climate

## 1. Introduction

The decoupling of buildings indoor climate from the surrounding environment to deliver essential thermal comfort for occupants consumes substantial amounts of energy and is one of the major contributors to climate change [1]. Today, increasing demand for buildings in many parts of the world has caused surges of electrical power demand particularly for space air conditioning. This is aggravated by heavy dependence on cheap and inefficient energy intensive mechanical air conditioning systems for thermal comfort. Therefore, the current focus is to develop thermal comfort solutions in buildings that can deliver net zero emission of greenhouse gases and other pollutants including high global warming potential refrigerants [2, 3]. Current mechanical air conditioning systems are expected to remain dominant while new and more sustainable solutions are being identified and developed [4]. The building sector worldwide contributes 40% of the total

45 primary energy consumption and the equivalent of 33% of the carbon emitted into the environment  
46 [5]. Therefore, in many parts of the world there is renewed awareness to address the high energy  
47 demands, through for example integration of passive cooling techniques in sustainable  
48 architectural designs [6].

49 Indeed, for many centuries, in regions of the world with hot and dry climates, traditional cooling  
50 methods such as evaporative cooling were exclusively used to keep buildings cool in summer  
51 temperatures. For example, across countries in the Middle East evaporative cooling in building  
52 using porous water jars in wind catchers was widely practiced [7]. Moreover, evaporative cooling  
53 has the potential to maintain effectively favourable comfort levels in modern buildings and  
54 dispense full requirement of fresh air. Being low intensive energy process, evaporative cooling  
55 can reduce peak electricity demand, save as much as 75% on energy consumption and reduce  
56 carbon emission by 44% compared to vapour-compression air-conditioning [8, 9]. The drawback  
57 of evaporative cooling, however, resides in cooling performance being strongly dependant on the  
58 ambient conditions of temperature and humidity, limiting the application scope of the technology  
59 [10-13].

60 Previous research has addressed the design and performance challenges of evaporative cooling  
61 system both analytically and experimentally. For instance, Kumar and his team [14] investigated  
62 the performance of an evaporative cooling unit for varying ambient conditions. The authors found  
63 that the unit performs better under dynamic conditions than static conditions. Da Veiga, Güths,  
64 and Da Silva [15] presented and experimentally tested a model to forecast the effectiveness of  
65 evaporative cooling as a method to limit excessive heat gain in buildings' roofs. In most tests, the  
66 model was able to forecast with high precision the heat flux passing through the porous medium.  
67 Under specific conditions, the performance of the wet porous media can exceed that of its dry  
68 counterpart. Kowalski and Kwiecie [16] investigated evaporative cooling (EC) systems for an  
69 imaginary Polish industrial building using the TRNSYS 17 software in which it evaluated six  
70 systems in four Polish cities (Koszalin, Lublin, Suwalki and Wroclaw). By generalising the results,  
71 EC systems may be able to conserve energy in Poland's climate. Lapisa and colleagues [17]  
72 discussed the layout of commercial building envelopes for low-rise structures. It presented a Multi  
73 objective optimisation using the NSGA-II approach to determine the ideal design parameters for  
74 passive cooling solutions such as cool roofs and nighttime natural ventilation. Alshenaifi et al. [18]  
75 proposed a creative setup with three air outlet disposition of a passive downdraught evaporative  
76 cooling (PDEC) tower to be investigated numerically using CFD (Computational Fluid Dynamics)  
77 software; based on the findings, the input velocity and temperature had a substantial impact on  
78 the quality of the interior temperature. Furthermore, He, et al. [19] discussed a solar-powered reel

79 dehumidifying system for evaporative cooling. Experimental tests showed that the system can  
 80 decrease the indoor temperature and maintain the relative humidity. Dhamneya, Rajput and Singh  
 81 [20] studied the performance of an evaporative cooling window air conditioner. The proposed  
 82 solution performs better, saving 7.39% of energy in April and 5.18% in March. Boukhanouf et al.  
 83 [21] proposed a heat pipe and porous ceramic tube regenerative evaporative cooler prototype. It  
 84 described the cooler's construction and lab findings. Experimental results show that the cooler air  
 85 supply temperature can be 14°C lower than ambient air.

86 Moosavi, Zandi, and Bidi [22] explored the cooling performance of a naturally ventilated house  
 87 with a solar chimney and hybrid evaporative cooling. The hybrid evaporative cooling system and  
 88 solar chimney lowered the atrium centre zone's air temperature by 0.7 °C. Leroux et al. [23]  
 89 presented an evaporative cooling system with a porous evaporator wall. Using a mathematical  
 90 model and an experimental setup, evaporator material properties and their effect on cooling  
 91 system performance were determined. The calculated evaporator wall power ranges from 12 to  
 92 72 W/m<sup>2</sup>. Zhang et al. [24] examined the influence of climatic factors on the evaporative cooling  
 93 of porous building materials. According to their findings, the factors that had the greatest influence  
 94 on the evaporative cooling process are the amount of solar radiation, the temperature of the air,  
 95 the partial pressure of the water vapour, and the speed of the wind.

96 Many study have shown that Evaporative coolers offer higher overall energy efficiency than  
 97 Vapour Mechanical Compression (MVC) system, particularly when deployed in favourable  
 98 climatic conditions. The MVC systems are effective in temperature and humidity control and stable  
 99 operation, but suffer from low Coefficient of Performance (COP) and sever adverse environmental  
 100 impact, compared to evaporative coolers as shown in Table 1 [25-27].



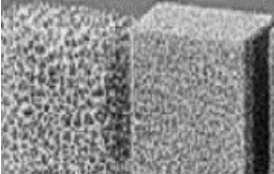
101 Table Error! No text of specified style in document. comparison between some air-conditioning  
 102 systems [25-27]

<b>System type</b>	<b>VMC cooling</b>	<b>Evaporative cooling</b>
<b>Property</b>		
<b>COP</b>	2 to 3	5 to 27
<b>Power consumption</b>	High	Medium/Low
<b>Refrigerants</b>	CFCs, HFCs	Water
<b>Environmental Impact</b>	High	Low

104 The concept of evaporative cooling involves a complex process of heat and mass transfer  
 105 between a wet surface and an air stream flowing immediately over it. The air stream, often warm  
 106 fresh air supply, loses its sensible heat in exchange for increased moisture content gained from  
 107 water evaporating off the wet surface. The cool air can be supplied directly to buildings (DEC) to  
 108 displace warm air or used to cool indirectly (IEC) through a heat exchanger air supply to buildings  
 109 [7]. The main advantage of IEC is that its air humidity can be controlled separately [10].  
 110 One of the key components of an evaporative cooling system is the wet media material, which is  
 111 usually made of a porous structure of large surface area. The thermal properties of these materials  
 112 are characterised by their affinity to absorb and hold liquid water; as well as enable fast  
 113 evaporation [21, 28]. There are many types of materials used as wet media in evaporative coolers  
 114 including metals foams, organic and synthetic fibres, and porous ceramics. Research works into  
 115 these types of materials and their properties are summarised in Table 2.

116

117 **Table 2:** Types and properties of evaporative coolers wet media materials [8, 29, 30]

Material type	characteristics	structure
<b>Organic fibres (Randomly packed wet pads)</b>	<ul style="list-style-type: none"> <li>• made from shredded organic matter fibres</li> <li>• have good water absorption properties</li> <li>• low thermal conductivity</li> <li>• high porosity (&gt;50%)</li> </ul>	
<b>Cellulose (rigid cardboard box/kraft paper)</b>	<ul style="list-style-type: none"> <li>• takes the form of rigid or corrugated paper</li> <li>• thermal properties can vary depending on the specific material and packing</li> <li>• Offers enhanced water evaporation</li> </ul>	
<b>Standard randomly packed metal fibre wet pads</b>	<ul style="list-style-type: none"> <li>• high strength, low density, and thermal conductivity</li> <li>• made from copper, aluminium, and steel</li> <li>• The porosities range from 30–95% and depends on metal fibre length, fibre diameter, and the density</li> </ul>	

**Porous ceramic**

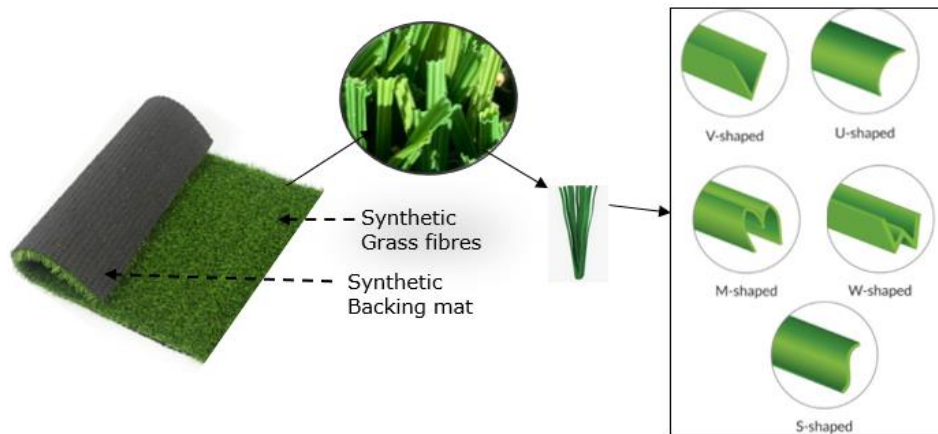
- Have high thermal conductivity
- Have large contact area and uniform water distribution
- Durable and high water-retention capacity
- Porosity depends on production temperatures (at baking temperature of 1250° C, a bulk porosity of 47% was reported)



118

119 This paper introduces synthetic grass as wet media material in the form of flat mat sheets,  
120 commonly used in sport fields, landscaping, playgrounds, etc. These synthetic grass sheets are  
121 manufactured from plastics such as Polyethylene (PE) or Polypropylene (PP) and are structurally  
122 stable under wet conditions, high ambient temperatures, and UV exposure [31, 32].

123 The Synthetic grass fibres are implanted in a back support mat, which is also made of a  
124 combination of polypropylene and polyethylene. The back mat is coated with latex to hold the  
125 grass fibres in place and provide rigidity. The synthetic grass fibres are then cut to required height  
126 [33]. Figure 1 shows the form of grass mats, the backing material and the type of grass fibre  
127 shapes.



128

129 **Figure 1:** Sample synthetic grass sheet and fibre forms

130

131 **1.1 Research gap and contribution**

132 The adoption of synthetic grass mats in evaporative cooling systems can potentially contribute to  
133 increasing service-life span and minimising the requirement for maintenance. Synthetic grass  
134 fibres are made in various shapes to provide large wet surface area and air contact for enhanced  
135 evaporation process, are readily available and at low production cost. The synthetic grass mats  
136 can be installed in new or as replacement in evaporative cooling systems. Unlike organic wet  
137 media materials used in evaporative cooling systems, synthetic grass mat rolls do not require  
138 water or fertilizers to cultivate and are recyclable [31]. This work aims to evaluate experimentally

139 this novel wet media material which is produced as a synthetic grass mat in three types of  
 140 evaporative coolers: Direct Evaporative Cooling (DEC), Indirect Evaporative Cooling (IEC), and  
 141 Dew point evaporative cooling (DPEC). A comparative performance analysis, in terms of system  
 142 effectiveness and cooling capacity, with similar published data of evaporative coolers was also  
 143 conducted.

144

145 **1.2 Target climatic condition for evaporative cooling**

146 A further contribution of this research is to support the development and adoption of evaporative  
 147 cooling systems as a sustainable solution to thermal comfort in buildings in hot and dry climate  
 148 such as the arid and semi-arid regions of the world. These regions are characterised by extreme  
 149 conditions of long and hot summers with temperatures often exceeding 40° C, and minimal  
 150 precipitation. The average atmospheric temperatures has also been noticeably increasing due to  
 151 climate change [34]. For example, many cities across the Middle East (Riyadh, Baghdad, Kuwait,  
 152 etc.) routinely experience intense heat, with temperatures occasionally surpassing 50° C. Figure  
 153 2 illustrate prevailing average and maximum temperature and mean relative humidity in the city  
 154 of Riyadh, KSA [35], where the deployment of air conditioning in buildings due to high temperature  
 155 and low relative humidity (RH) lasts from April to October.

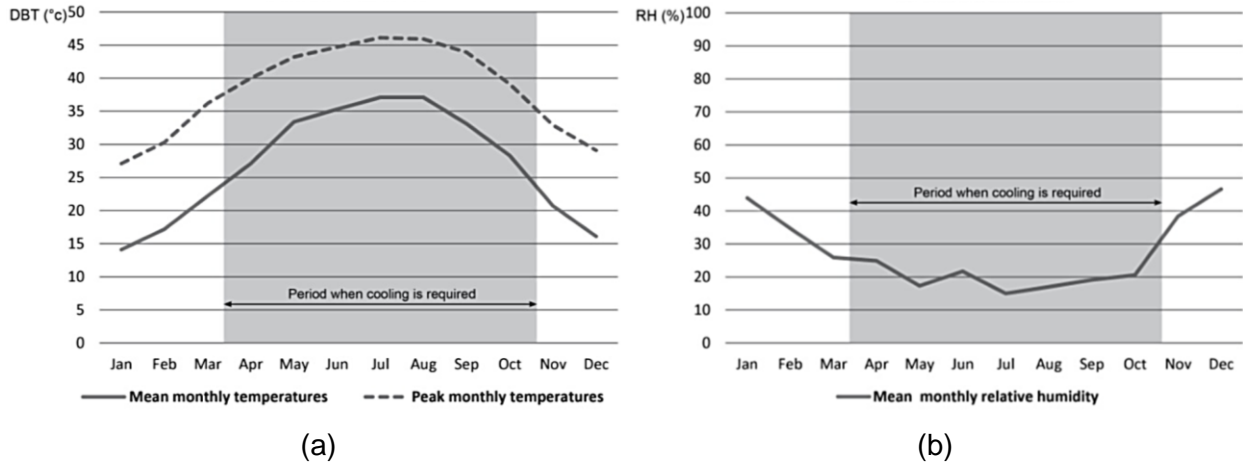


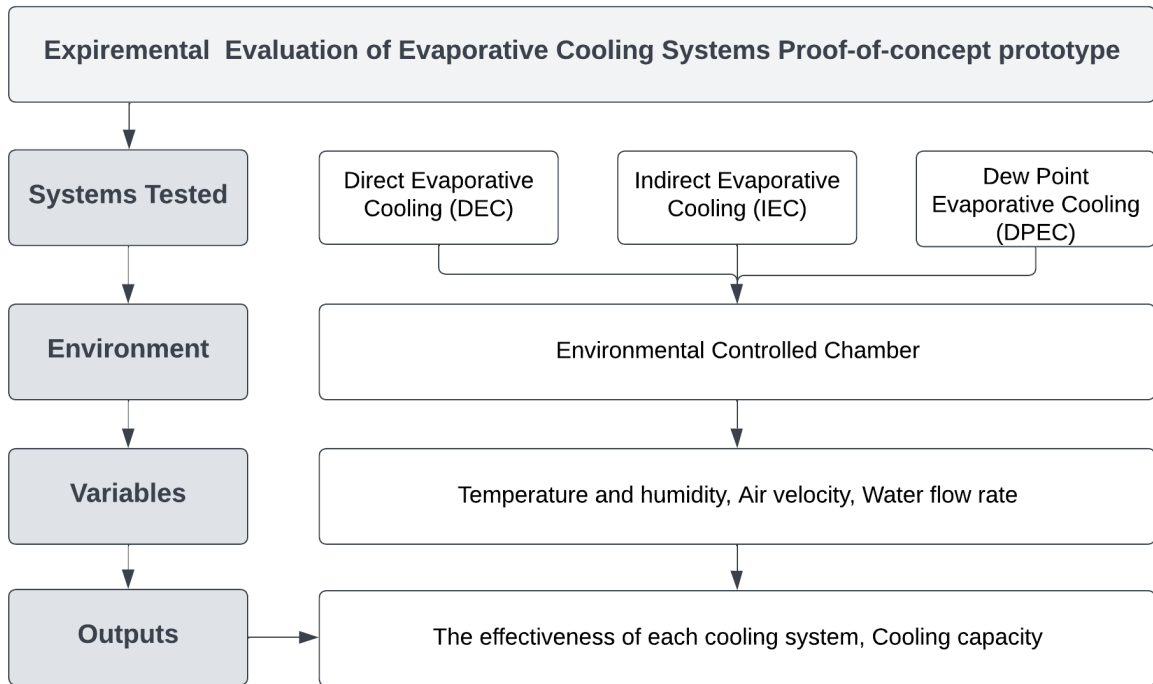
Figure 2: Typical weather condition in city of Riyadh, KSA (a) Monthly Average and maximum air temperature (b) monthly mean RH

156 **2. Methodology**

157

158 The energy performance of a laboratory prototype evaporative cooler using synthetic grass fibres  
 159 was evaluated under controlled climatic conditions. The experimental work made use of an  
 160 environmental chamber, which enabled the precise control of the temperature and relative

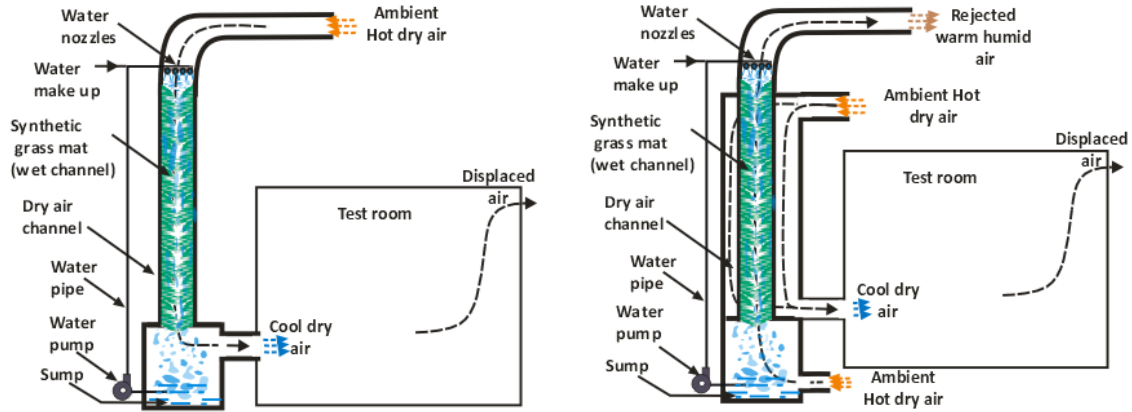
161 humidity (RH) of the air introduced into the prototype. The test conditions were set to span the  
 162 wider outdoor temperature range prevailing in hot dry climates such as that of Middle East. To  
 163 establish full performance of the synthetic grass media material, three configuration of evaporative  
 164 cooling systems were considered namely Direct Evaporative Cooling (DEC), Indirect Evaporative  
 165 Cooling (IEC), and Dew Point Evaporative Cooling (DPEC). Figure 3 gives an outline of the  
 166 research methodology used to evaluate the performance of the experimental coolers.



167  
 168 **Figure 3:** Schematic representation of the experimental method  
 169

170 **2.1 Description of the Evaporative cooling system configurations**  
 171

172 Each of the three configurations of evaporative cooling systems namely, Direct evaporative  
 173 cooling (DEC), Indirect evaporative cooling (IEC) and dew point evaporative cooling (DPEC)  
 174 requires a different mechanical arrangement and layout of the airflow channels. Figure 4 shows  
 175 a schematic arrangement of the airflow channels of the three evaporative cooling systems.  
 176

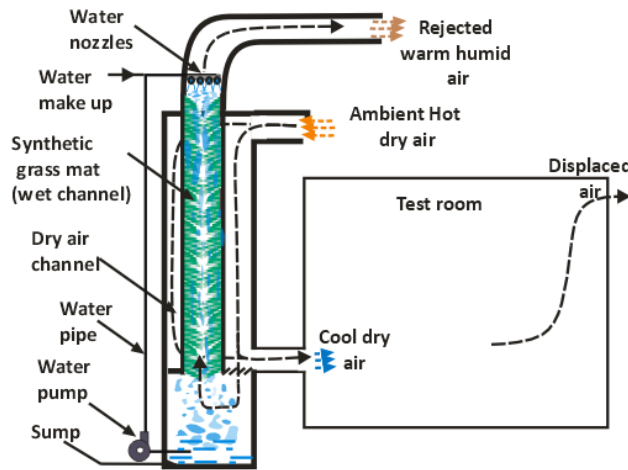


177

178

(a) Direct Evaporative Cooling (DEC)

(b) Indirect Evaporative Cooling (IEC)



179

180

(c) Dew point evaporative cooling (DPEC)

181

**Figure 4:** Arrangement of tested evaporative cooling systems

182

### 2.1.1 Direct Evaporative Cooling (DEC)

184

In the DEC mode, the hot dry ambient air inlet is located at the top opening of the tower that houses the synthetic grass media. The ambient air flows through the free-passages in the wet media and fully brought into contact with sprayed water at the top of the wet channel. The cool and saturated air is then supplied to the test room, which is cooled through displacement ventilation. The supply air temperature of this system is limited to the wet bulb temperature. The excess water (i.e., not evaporated) is collected in a sump below the wet channel and recirculated by a water pump, as shown in Figure 4 (a).

191

192

### 2.1.2 Indirect Evaporative Cooling (DEC)



193 For the IEC mode, the airflow through the cooler is arranged into two separate channels,  
194 the wet and dry channel, which shares a heat transfer surface area. The ambient air is  
195 drawn into the wet and dry channels at two separate inlets. The ambient air admitted into  
196 the wet channel undergoes cooling through direct evaporation and is rejected to outside  
197 as warm and humid air. Concurrently, the ambient air drawn in through the dry channel  
198 inlet is cooled by transferring its sensible heat to the cool wet channel wall surface and is  
199 supplied into the test room for displacement ventilation. This arrangement has the  
200 advantage of supplying cooled air, without increasing its humidity. Like the DEC  
201 arrangement, excess water leaving the wet channel is collected in the sump and is  
202 recirculated by a water pump, as shown in Figure 4 (b).

203

### 204 **2.1.3 Dew point evaporative cooling (DPEC)**

205 The mechanical arrangement of airflow in the DPEC mode is similar to that of the IEC  
206 mode, as it employs separate dry and wet channels. However, in the DPEC mode,  
207 approximately 50% of the airflow from the outlet of the dry channel is redirected into the  
208 wet channel for the evaporation process as it comes into contact the wet synthetic grass  
209 media. The remaining cool and dry air from the dry channel is supplied to the test room  
210 for displacement ventilation. This allows the air supplied into the test room to be cooled to  
211 a temperature approaching the ambient air dew point temperature without increasing its  
212 moisture content. To control the amount of cool and dry air supply to the test room, a  
213 damper was placed at the inlet of the wet channel. Figure 4(c) shows the airflow  
214 arrangement of the DPEC mode.

215

## 216 **2.2 Laboratory rig set up**

217 The core of the evaporative cooling system is the synthetic grass wet media module, as shown in  
218 Figure 5 (a). The module is made of multiple layers of grass mat backed by a thin aluminium plate  
219 for rigidity. The synthetic grass mats were then stacked vertically and separated by an air gap to  
220 allow airflow in between. Depending on the mode of operation of the evaporative cooling, the  
221 channels formed by the synthetic grass mats and the Aluminium back plate were arranged to  
222 allow for water and air direct contact (DEC) or wet and dry channels being separated to allow for  
223 indirect air cooling to take place, as explained previously. Table 3 summarises the main dimension  
224 of the core module.

225

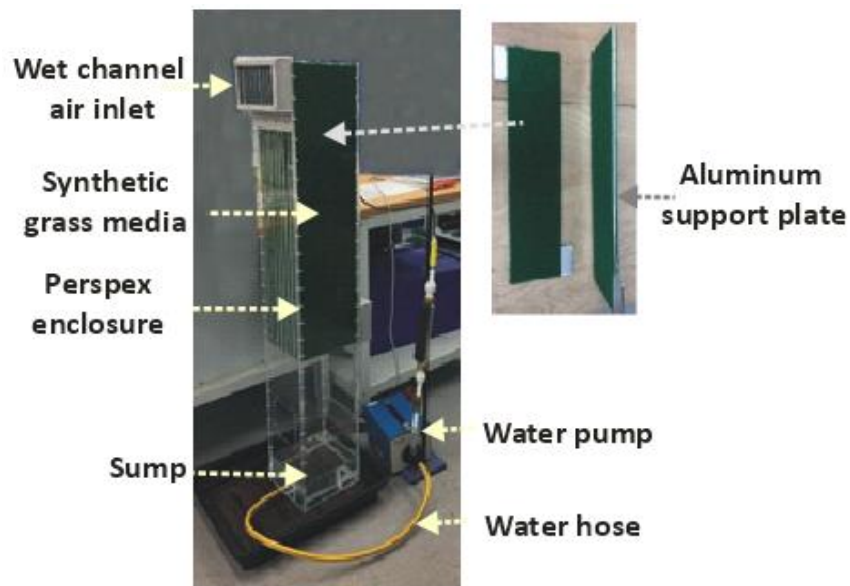
**Table 3:** Design parameters of the synthetic grass module

	Height (mm)	Width (mm)	Thickness (mm)	Number of layers (-)	Separation gap (mm)
<b>Synthetic grass mat</b>	800	800	3	9	-
<b>Backing aluminum plate</b>	200	200	1	5	-
<b>Dry channel inlet/outlet</b>	100	5	-	-	5
<b>Wet channel inlet/outlet</b>	100	5	-	-	3

226

227 The full test rig onto which the synthetic grass module is integrated was then placed on a wheeled  
 228 bench to be freely moveable into the environmental chamber in the laboratory for testing under  
 229 controlled temperature and relative humidity conditions. Figure 5 (b, c) shows the back and front  
 230 view of the test rig with the dummy cooled test room connected to the cooler using a flexible duct.  
 231

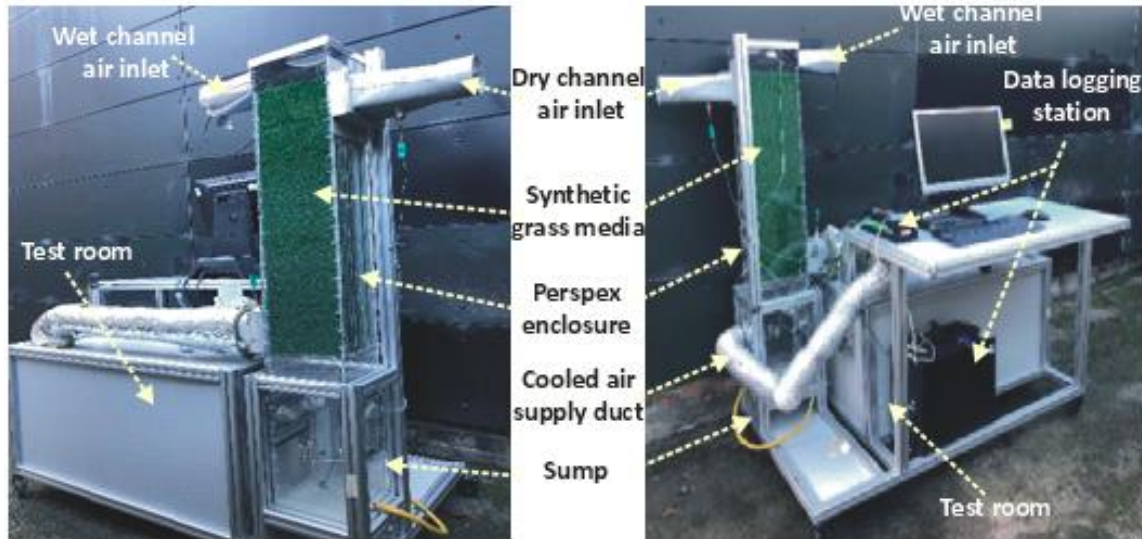
231



(a)

232

233






(b) (c)

**Figure 5:** Experimental set-up test rig a) synthetic grass fibres module (b) back view (c) front view

Furthermore, the test rig was equipped with thermocouples to measure airflow temperatures, anemometer to measure airflow velocities and hygrometer to measure air humidity at the inlets and outlets of the dry and wet channels. A data logging station was used to record measured parameters at fixed time intervals. A summary of the type of instrument and their specification used in the experiment is given in Table 4.

**Table 4:** Type of instrument and data logging

Instrument type	Description of use	Illustration
K-type thermocouples Range: --75 to +250° C Accuracy: +/- 2.2° C	located in the centre of the air flow passages to measure the temperature	
RS-232 humidity and temperature meters Temperature range: 0 to 60° C RH range: 0-95% Accuracy: ±3% RH and ±0.8 °C	Used to measure air temperature and humidity of the inlet and outlet of the dry and wet channel	
Testo 405- V1 hotwire anemometer Temperature Range: 0 to 50° C Accuracy: ±0.5° C and ±0.3 m/s + 5% Measured value	Testo 405- V1 is a portable hotwire anemometer used to measure the flow velocity at the inlet and exit of the dry and wet channel	

Data logger, data-taker model  
DT500, Series 2

Logs temperature readings from the  
thermocouples and humidity at fixed  
time interval and stored data is  
retrieved for analysis.



Centrifugal liquid Pump- Model C16-  
C Charles Austen  
220-240 V, 0.25 A, 50 Hz

Water circulating pump



Ventilation inline-fan  
Vent-axia 220-240 V, 0.21 A, 50 Hz

Air circulating fan



244

### 245 2.3 Performance indices

246

247 The measured operating parameters of the three evaporative coolers were used to calculate the  
248 cooling performance in terms of cooling effectiveness, potential cooling capacity and COP. These  
249 energy performance indices can be used to compare and identify the most effective cooling  
250 solutions for a given application. The cooling effectiveness of the system was evaluated using the  
251 wet bulb effectiveness which is the ratio of the difference between ambient air temperature and  
252 the supply air temperature to the difference between the ambient air temperature and its  
253 corresponding wet-bulb temperature. The wet bulb effectiveness is expressed by the following  
254 formula:

$$255 \quad \varepsilon = \frac{T_{in} - T_s}{T_{in} - T_{wb}} \quad (1)$$

256 Where;  $\varepsilon$  is the wet bulb effectiveness of cooler;  $T_{in}$ : the Inlet ambient dry bulb temperature ( $^{\circ}\text{C}$ ),  
257  $T_s$ : the supply temperature ( $^{\circ}\text{C}$ ) and  $T_{wb}$ : the inlet wet-bulb temperature ( $^{\circ}\text{C}$ ). Similarly, the Cooling  
258 capacity,  $Q_c$ , of the evaporative cooler is expressed as follows:

$$259 \quad Q_c = \dot{m}c_p(T_{in} - T_s) \quad (2)$$

260 where,  $\dot{m}$  is the mass flow rate (kg/s),  $c_p$  is the specific heat capacity of air ( $\text{J}/\text{kg}\cdot^{\circ}\text{C}$ ),  $T_{in}$  is the  
261 inlet dry bulb temperature ( $^{\circ}\text{C}$ ) and  $T_s$  is the supply dry bulb temperature ( $^{\circ}\text{C}$ ). The other important  
262 performance index is the coefficient of performance (COP) of the evaporative cooler. The COP is  
263 the ratio between the cooling capacity of a cooler and the power demand to operate the cooler,  
264 which in this case is represented by the power load of the water pump and air circulating fan. It  
265 can be written as:

$$266 \quad COP = \frac{Q_c}{P_p + P_f} \quad (3)$$

267 where,  $Q_c$  (W) is the cooling capacity,  $P_w$  (W) and  $P_f$  (W) are the water pump and fan power  
268 demand. However, in this study, the power demand of the auxiliary equipment (the water pump  
269 and ventilation fan) were not optimised, and the COP calculation doesn't provide a precise  
270 representation of the energy performance of evaporative coolers.

271 However, in this work, the power demand of the auxiliary equipment (the water pump and  
272 ventilation fan) were not optimised and the COP calculation doesn't give an accurate picture of  
273 the evaporative coolers energy performance.

274 The final important parameters measured in this work is the water consumption rate of the  
275 evaporative coolers. The water consumption rate of an evaporative cooler depends on mainly  
276 on airflow rate in contact with the wet surface and the inlet and outlet moisture content of  
277 the air. This can be calculated by the following equation [25]:

$$278 \quad \dot{V}_w = \frac{\dot{V}_a \rho_a}{\rho_w} (w_{a,out} - w_{a,in}) \quad (4)$$

279 where,  $\dot{V}_w$  is the water evaporation (consumption) rate,  $\text{m}^3/\text{s}$ ;  $\dot{V}_a$ : air flow rate in the wet  
280 channel,  $\text{m}^3/\text{s}$ ;  $\rho_a$  is the air density,  $\text{kg}/\text{m}^3$ ;  $\rho_w$  is water density,  $\text{kg}/\text{m}^3$ ;  $w_{a,out}$  is the moisture  
281 content of the outlet air,  $\text{kg}/\text{kg}_{\text{dry air}}$ ; and  $w_{a,in}$  is the moisture content of the inlet air,  
282  $\text{kg}/\text{kg}_{\text{dry air}}$ .

## 283 **2.4 Experimental testing conditions**

284  
285 It is well established that evaporative cooling technology is more effective in hot and dry climates.  
286 Hence, the focus of this work was to evaluate the suitability of the evaporator cooling system for  
287 the climatic conditions such as those prevailing in Middle East region. As such, the energy  
288 performance of the cooling system was tested over a range of controlled ambient air dry bulb  
289 temperatures (30° C, 35° C, and 40° C) and air relative humidities (25, 35, and 45 %). The small-  
290 scale testing of the system focuses on displacement ventilation where air in the test room is  
291 constantly renewed and airflow rates appropriate for this mode of cooling were selected. For  
292 example, the maximum airflow velocity for direct, indirect, and dew point evaporative cooling were  
293 2.85, 1.65, and 1.85 m/s, respectively.

294 Similarly, the evaporative cooling effect consumes water through evaporation as it is brought in  
295 direct contact with air. The water is sprayed through nozzles on the grass fibres from the top of  
296 the wet channels and any excess water is accumulated in the sump and continuously recirculated.  
297 A water flow rate of 0.5  $\text{m}^3/\text{minute}$  was selected as it provides maximum wettability of the synthetic  
298 grass fibres surface and minimum requirement for water recirculation.

299

### 300 3. Results and Discussion

301

#### 302 3.1 Direct evaporative cooling (DEC) Configuration

303

304 In a direct evaporative cooling mode, the supply of air into occupied space is channelled through  
305 a wet channel and cooled to near its moisture saturation wet bulb temperature. This mode of  
306 operation may be necessary when the ambient air is very dry and the addition of moisture into  
307 the occupied space is required. The thermal performance of the laboratory synthetic grass fibres  
308 in direct cooling mode was evaluated at temperatures of 30, 35 and 40°C and at corresponding  
309 RH of 25, 35 and 45% with inlet air velocity of 2.85 m/s. The supply air is drawn in into the test  
310 room through the cooler wet channels.

311

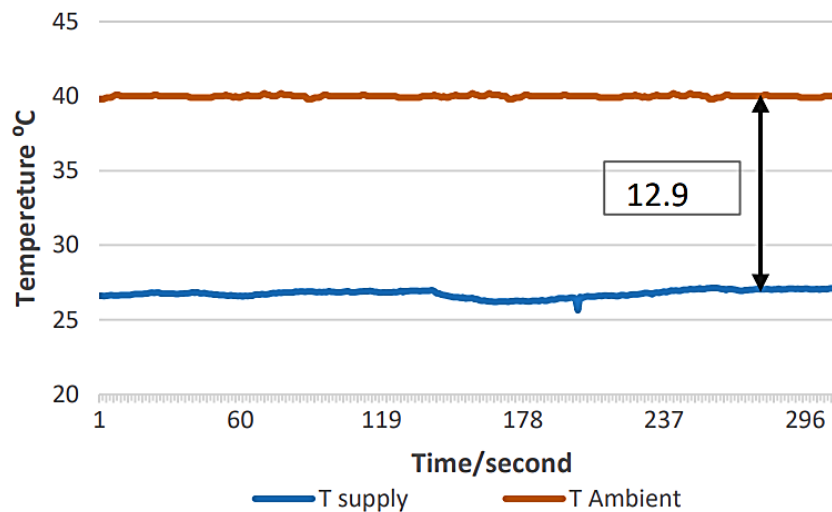
##### 312 3.1.1 Cooling performance

313

314 Under steady state operating condition of ambient inlet air temperature of 40° C and relative  
315 humidity of 30.9%, the air temperature of supplied air decreased to 27.1° C, a 12.9° C drop, as  
316 shown in Figure 6.

317

318



319

320

321 **Figure 6:** Steady state DEC inlet and supply air temperature (RH: 30.9%, airflow velocity: 2.85  
322 m/s))

323

324 The overall steady state cooling performance of the direct evaporative cooler is summarised in  
 325 Table 5. It is shown that the supply air temperature decreased to within 2° C of the wet bulb  
 326 temperature (25.3° C) and its RH approaches full saturation (90.6%). In addition, the wet bulb  
 327 effectiveness and cooling capacity of the DEC was estimated to be 87.7 % and 339.57 W,  
 328 respectively.

329  
 330

**Table 5:** DEC mode operating parameters

Velocity Inlet Air	Mass flow rate	RH Inlet Air	Temp Inlet Air	Temp Supply air DB	Temp Supply air WB	Temp Supply air DP	RH Supply air	Effectiv ness	COP	Cooling capacity
(m/s)	(kg/s)	(%)	(°C)	(°C)	(°C)	(°C)	(%)	(-)	(-)	(W)
2.85	0.027	30.9	40	27.1	25.3	19.61	90.6	0.877	3.20	339.57

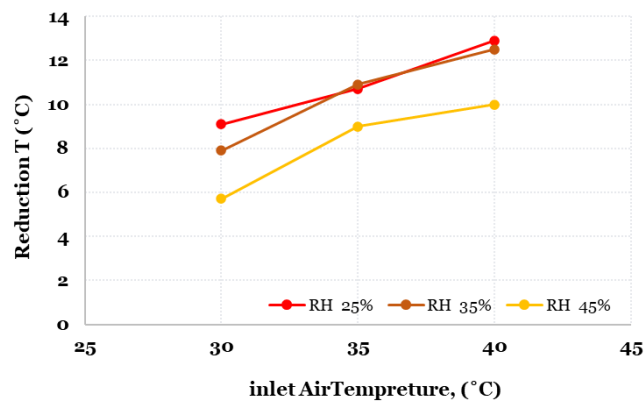
331

332 *3.1.2 Effect of inlet air temperature and RH on air supply temperature*

333

334 The measured temperature of the DEC, shown in Figure 7, supports the general understanding  
 335 that the effectiveness of direct evaporative cooling is favoured when ambient temperature is  
 336 high, and RH is low. As discussed previously, at steady state operation of ambient inlet air at  
 337 40°C and 25% RH, a temperature drop of 12.9°C was achieved; whereas at the same  
 338 temperature and RH of 45%, the inlet air temperature reduction was only 10° C. The lowest  
 339 value temperature drop (of 5.7° C) was recorded for inlet air of 30° C. Therefore, the  
 340 temperature drop of the inlet air through the cooler improved as the ambient air temperature  
 341 increased. This represents an advantage of evaporative coolers over mechanical vapour  
 342 compression cooling systems.

343



344

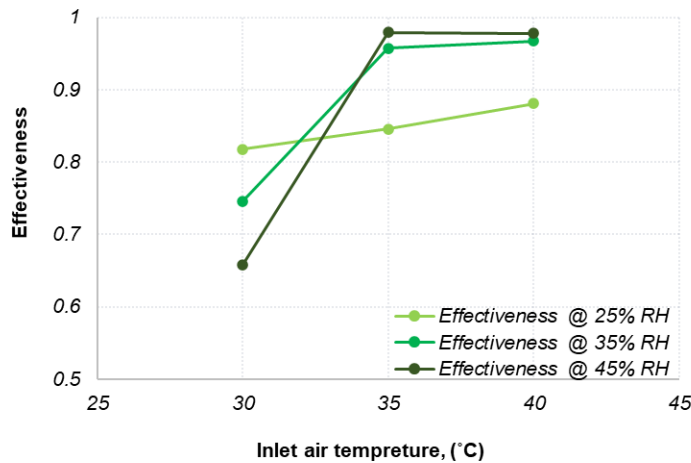
**Figure 7:** Supply air temperature drop (airflow velocity: 2.85 m/s)

345

346 *3.1.3 Effect of inlet air temperature and RH on effectiveness*

347

348 The effectiveness of the system was calculated using the wet bulb effectiveness formula  
 349 given in Equation 1. The effect of ambient air temperature on the effectiveness of the DEC  
 350 system was further evaluated at different temperatures and RH. As illustrated in Figure 8, the  
 351 effectiveness of the DEC cooling system increased as the inlet ambient air temperature rose.  
 352 The highest effectiveness peaked at 0.97, at inlet temperatures of 40° C and 45% RH, which  
 353 is very close to the maximum limit of 100%. However, the effect of RH on the system  
 354 effectiveness was less pronounced, as increasing ambient air RH had the opposite effect on  
 355 the trend of cooling effectiveness.



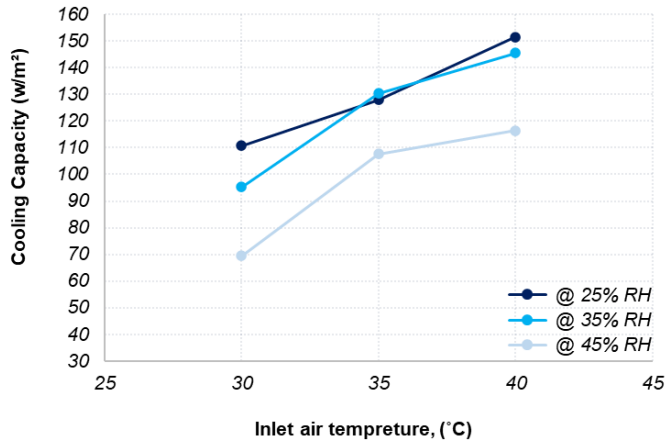
356  
 357 **Figure 8:** Effectiveness of DEC (airflow velocity: 2.85 m/s)

358  
 359 3.1.4 Effect of inlet temperature and RH on cooling capacity

360 In this work, the cooling capacity of the DEC system was presented relative to the synthetic  
 361 grass fibres surface area. The effect of ambient air temperature and RH on cooling capacity  
 362 is presented in Figure 9. This shows that the cooling capacity increases with increasing  
 363 ambient air temperature. For example, for ambient air RH of 25%, the cooling capacity  
 364 increased by about 27% (from 110.76 to 151.59 W/m<sup>2</sup>) when the ambient air temperature  
 365 increased from 30° C to 40° C. Equally, a similar improved cooling capacity trend can be  
 366 observed for ambient air RH of 35 and 45%.

367 However, the cooling capacity of the cooler declined as the ambient air RH increased from  
 368 25 to 45%. This is a result of a drop in temperature difference between that of ambient air  
 369 and cooled supply air. For example, at ambient air temperature of 40° C, the cooling capacity  
 370 declined by about 20% as RH of the inlet air rose from 25 to 45%.  
 371





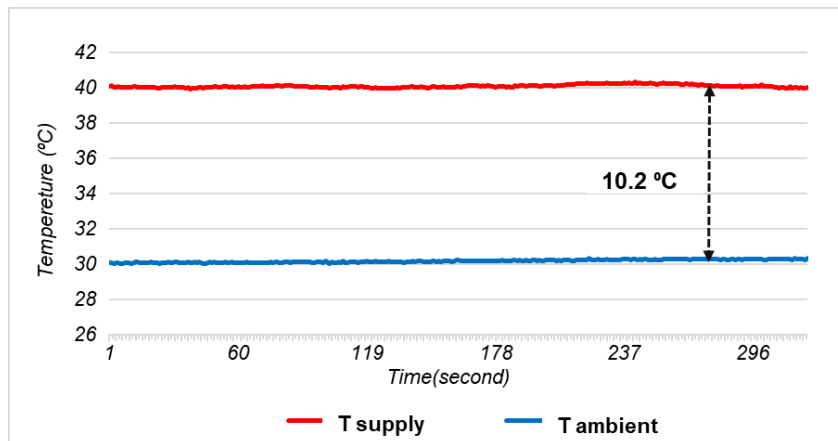
372  
373 **Figure 9:** Cooling Capacity DEC (airflow velocity: 2.85 m/s)

374  
375 **3.2 Indirect evaporative cooling (IEC) Configuration**

376 In this arrangement, the hot dry inlet air was forced through the dry channels into the occupied  
377 space. Equally, the ambient air was circulated through the wet channel to perform water  
378 evaporation and cool the air. The airflow in the dry channel is then cooling indirectly by transferring  
379 heat through the thin aluminium support plate separating the two channels. The optimisation of  
380 heat transfer process between the two airflows was not the subject of this work.

381  
382 **3.2.1 Cooling performance**

383 Figure 10 show a selected steady state inlet and supply air temperature, which shows the IEC  
384 cooler maintains a temperature difference of 10.2° C.



385  
386 **Figure 10:** Steady state IEC inlet and supply air temperature (airflow RH: 29.1% and velocity:  
387 1.65 m/s)

388

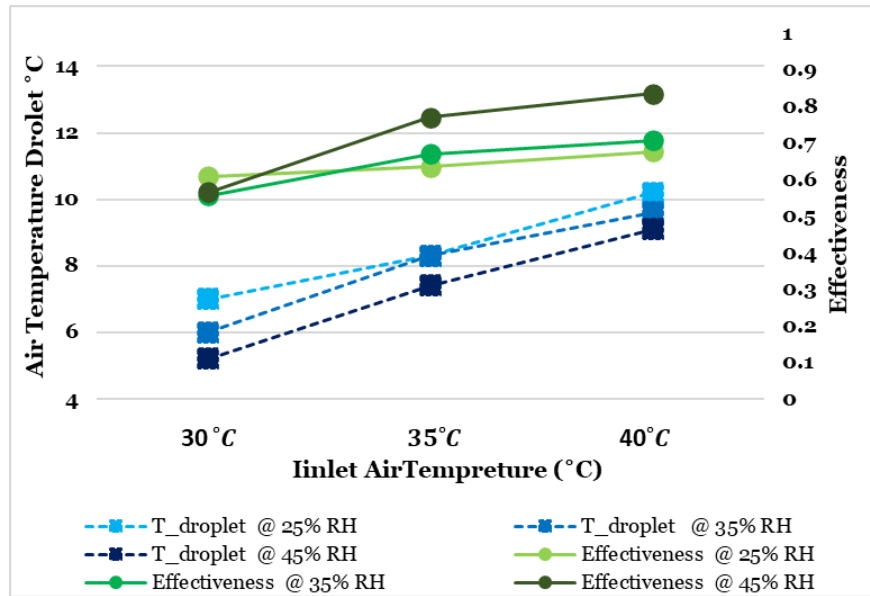
389 A summary of the measured steady state temperatures, calculated effectiveness and cooling  
 390 capacity is also presented in Table 5.

391  
 392 **Table 1:** Measured steady state performance parameters in the IEC Configuration

Velocity Inlet Air	RH Dry channel	Temp Inlet Channel	Temp Dry Supply DB	Temp Inlet WB	Temp Inlet DP	Temp Inlet wet channel	Temp Outlet wet channel	RH Outlet wet channel	Calculated effectiveness	COP	Calculated cooling capacity
m/s	%	°C	°C	°C	°C	°C	°C	%	(-)	(-)	W
1.65	29.1	40.5	30.3	25.4	19.09	40.5	32.1	87.7	0.67	1.47	155.4

394  
 395 **3.2.2 Effect of ambient air temperature and RH on supply air temperature and**  
 396 **cooling effectiveness**  
 397

398 The temperature drop through the IEC at ambient air temperature of 30, 35 and 40° C and  
 399 corresponding RH of 25, 35 and 45% while the airflow rate was maintained at 1.65 m/s are  
 400 presented in Figure 11. Likewise, this shows the highest temperature drops are yielded at higher  
 401 ambient temperature and lower air RH. For instance, at ambient air temperature of 40° C and  
 402 25% RH, the airflow temperature decreased by 10.2° C.  
 403



404  
 405  
 406 **Figure 11:** IEC cooler Effectiveness and air temperature drop (airflow velocity: 1.65 m/s)

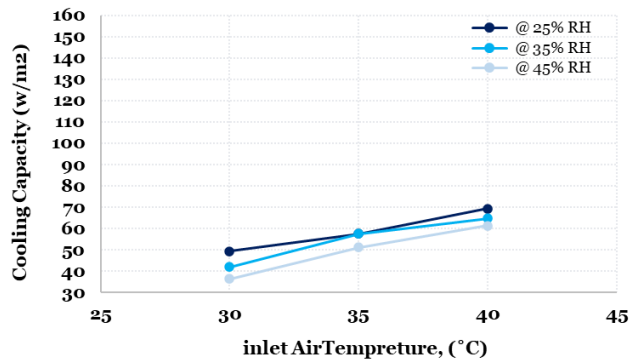
407  
 408 In addition, Figure 11 shows the effect on the effectiveness of the IEC system follows a similar  
 409 trend in that high effectiveness was achieved at high ambient inlet temperature and lower RH.

410 For instance, the effectiveness of the cooler increased from 0.56 to 0.85 for ambient inlet  
411 temperature increase from 30° C to 45° C at constant RH of 45% and airflow velocity of 1.65 m/s.

### 412 3.2.3 Effect of ambient inlet temperature and RH on cooling capacity

413  
414 The influence of ambient air temperature and RH on the cooling capacity of the cooler is shown  
415 in Figure 12. This shows that the cooling capacity of the IEC increases with increasing ambient  
416 inlet-air temperature. Conversely, the cooling capacity decreases with increasing air RH. For  
417 instance, at inlet air RH of 25%, the cooling capacity increased from 49.4 to 69.39 W/m<sup>2</sup> as inlet  
418 air temperature increased from 30 to 40°C. In contrast, at ambient inlet temperature of 30° C, the  
419 cooling capacity decreased from 49.4 to 31.5 W/m<sup>2</sup>.

420



421

422 **Figure 12:** IEC cooler system Cooling capacity (airflow velocity: 1.65 m/s)

423

### 424 3.3 Dewpoint evaporative cooling operation mode

425

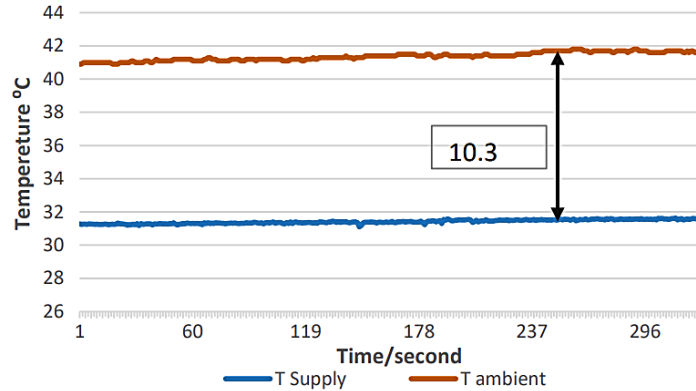
426 DPEC coolers have the advantage of supplying cooled air at temperature below wet bulb  
427 temperature of ambient inlet air by sacrificing a portion (up to 50%) of the dry channel cool outlet  
428 air for doing the evaporation work in the wet channel.

429

#### 430 3.3.1 Cooling performance

431 Like in the previous cases, the steady state inlet and supply air temperature of the DPEC was  
432 recorded, as shown in Figure 13. The cooler maintains an operating temperature difference of  
433 10.3° C when the inlet air temperature and RH are held at 41.8° C and 27.4%, respectively.

434



435  
436  
437  
438

**Figure 13:** Steady state DPEC inlet and supply air temperature (RH: 27.4% and airflow velocity: 1.85 m/s)

439  
440  
441  
442  
443  
444  
445  
446

Further details of measured operating parameters of the DPEC are summarised in Table 6. This shows that supply air temperature (31.5° C) is higher than the ambient air wet bulb temperature (25.5 °C), which indicates that the cooler did not achieve the sub wet bulb temperature condition. Equally, the wet bulb effectiveness and cooling capacity were 0.67 and 174.4 W respectively. A full optimisation of the design to operate in this mode would be required to improve its performance and achieve cooling air temperature below the corresponding wet bulb temperatures.

447

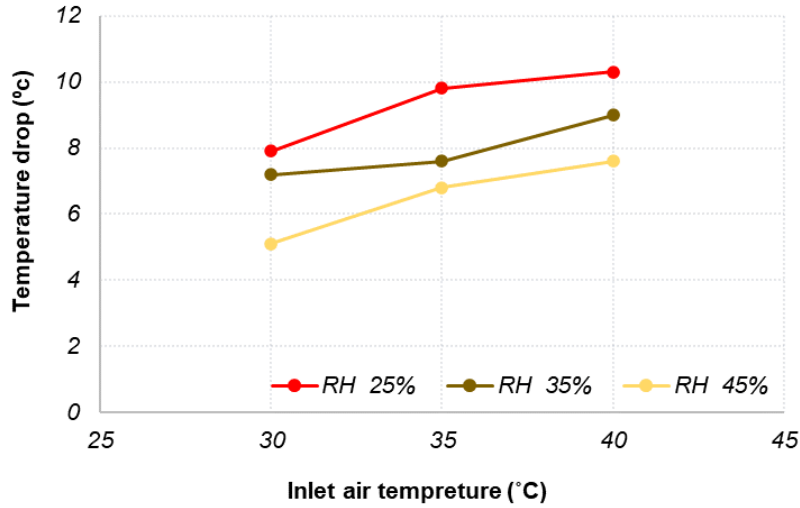
**Table 2:** Dewpoint evaporative cooling mode operating parameters

Velocity Inlet Air	RH Dry channel	Temp Inlet Channel	Temp Supply DB	Temp Inlet WB	Temp Inlet DP	Temp Inlet wet channel	Temp Outlet wet channel	RH Outlet wet channel	Calculated effectiveness	COP	Calculated cooling capacity
m/s	%	°C	°C	°C	°C	°C	°C	%	(-)		W
1.85	27.4	40.8	31.5	25.5	19.22	31.5	33.3	86.1	0.67	1.65	174.4

448  
449  
450  
451  
452  
453  
454  
455  
456

### 3.3.2 Effect of inlet air temperature and RH on supply air temperature

The effect of ambient air temperature and RH on the temperature of the air supply is shown in Figure 14. Similar trends to previous coolers arrangements were observed in this case too. For example, inlet ambient air temperature at 40° C and RH of 25, 35 and 45% achieved a drop in supply air temperature of 10.3, 9 and 7.6° C, respectively. Additionally, at ambient RH of 25% and temperature of 30, 35 and 40° C, the ambient air temperatures decreased by 10.3, 9.8 and 7.9° C, respectively.



457

458

**Figure 14:** Supply air temperature reduction (air velocity: 1.85 m/s)

459

### 3.3.3 Effect of inlet air temperature and RH on effectiveness

460

461

462

463

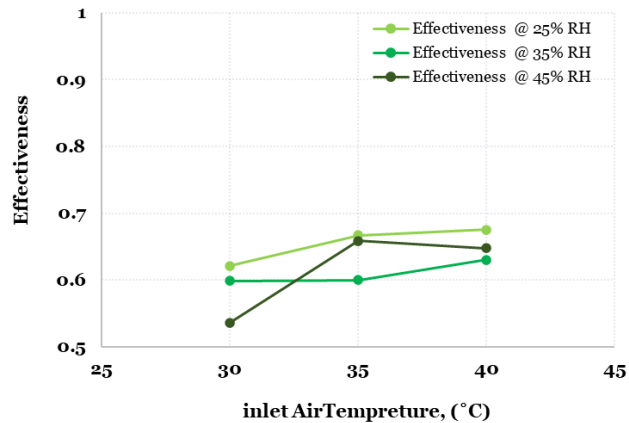
464

465

466

467

The effect of inlet air temperature and RH on the effectiveness of the cooling tower in DPEC mode is shown in Figure 15. The wet bulb effectiveness increases as the ambient air temperature increases. The highest wet bulb effectiveness is 0.67 at an ambient air temperature of 40° C, while the lowest value is 0.53 at 30° C. the effect ambient air RH however does not show a clear correlation.



468

469

470

**Figure 15:** Effectiveness of DPEC (airflow velocity: 1.85 m/s)

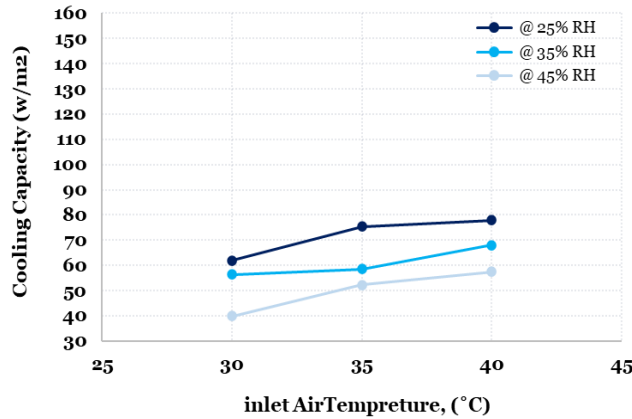
471

### 3.3.4 Effect of ambient inlet air temperature and RH on cooling capacity

472

473 The measured cooling capacity of the DPEC arrangement is illustrated in Figure 16. This shows  
474 that the cooling capacity increases as ambient air temperature increases. The maximum cooling  
475 capacity was achieved at 40° C and RH 25%.

476



477

478

**Figure 16:** Cooling Capacity DPEC cooler system

479 Likewise, it can be observed that the cooling capacity of the cooler increased as the air RH  
480 decreased. For example, the cooling capacity declined from 77.8 to 56.4W as ambient air RH  
481 decreased from 45% to 25 %.

482

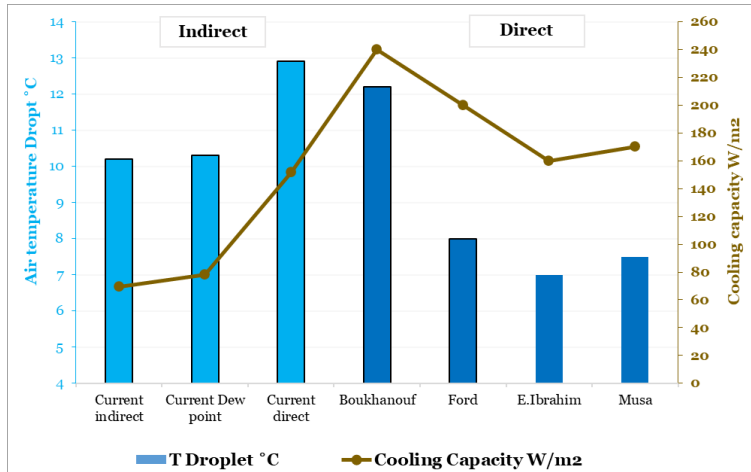
### 483 3.4 Comparative performance and Discussion

484

485 The experimental results compared the cooling capacity and supply air temperature reduction of  
486 three evaporative cooler designs using synthetic grass fibres as wet media, against published  
487 research by Musa [36], Ibrahim [37], Ford et al. [38] and Boukhanouf et al. [39]. These referenced  
488 works examined evaporative coolers with porous ceramic panels, as shown in Figure 17. The  
489 synthetic grass material used in this work produced higher cooling capacities and supply air  
490 temperature reduction in DEC cooling mode. However, in IEC and DPEC operating mode, the  
491 cooling capacity and air temperature performance is slightly lower than existing reported data.

492

493



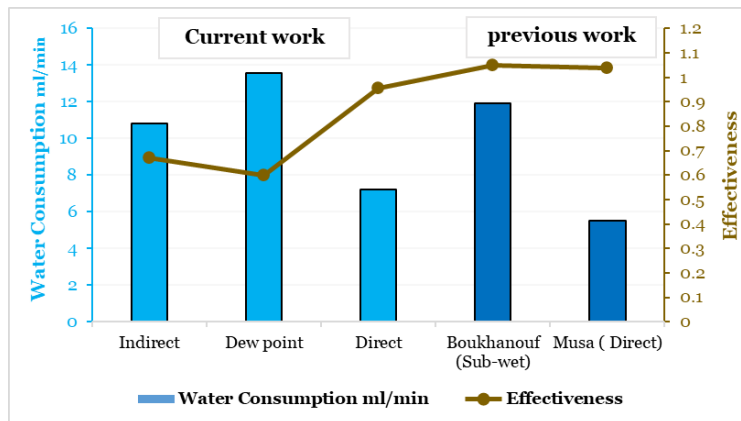
494

495 **Figure 17:** Comparison of experimental results of capacity and temperature drop (ambient air  
496 temperature: 40° C and RH: 25%

497

498 A further relevant comparison is evaluating water consumption of the synthetic grass wet media  
499 material and published work. Figure 18 shows that the proposed material has high water  
500 consumption rate and slightly lower effectiveness compared to previously reviewed works. The  
501 high-water consumption rate is mainly due to low water retention of synthetic grass fibres  
502 compared to low porosity ceramics or organic media. The synthetic grass fibres mats used in this  
503 work are designed for outdoor sport surface that allow fast drainage of rainwater.

504



505

506

507 **Figure 18:** comparison results of water consumption and effectiveness (ambient air  
508 temperature: 35°C and RH: 35%)

### 509 3.5 Uncertainty analysis

510

511 The reliability of the presented experimental data was further analysed considering the  
512 instruments and sensors individual precision and combining them to estimate the overall

513 uncertainty of the calculated key performance indices. This is critical for the consistency and  
 514 reproducibility of measurements under identical conditions. The respective uncertainty of the  
 515 calculated effectiveness and cooling capacity can be expressed as [40]:

516

$$517 \frac{e_{\varepsilon_{wb}}}{\varepsilon_{wb}} = \sqrt{\left(\frac{e_{T_{in}}}{T_{in}}\right)^2 + \left(\frac{e_{T_s}}{T_s}\right)^2 + \left(\frac{e_{T_{wb}}}{T_{wb}}\right)^2} \quad (5)$$

518

$$519 \frac{e_{Q_c}}{Q_c} = \sqrt{\left(\frac{e_{T_{in}}}{T_{in}}\right)^2 + \left(\frac{e_{T_s}}{T_s}\right)^2 + \left(\frac{e_v}{v}\right)^2} \quad (6)$$

520

521 where  $e$  is the thermocouple accuracy error,  $T$  is the measured temperature,  $e_v$  is the velocity  
 522 reading accuracy error, and  $v$  is the measured velocity.

523 The results of the uncertainty calculation are given in Table 7. The results show that the relative  
 524 uncertainty of effectiveness ranges from 3.04 to 3.23% indicating acceptable level of precision of  
 525 the measured results of the three evaporative coolers. The relative uncertainty of calculating the  
 526 cooling capacity was however slightly high ranging from 10.76 to 18.30%. This is greatly  
 527 influenced by the accuracy ( $\pm 0.3$  m/s) of the instrument used to measure the airflow velocity in  
 528 the air ducts and the difficulty in obtaining a uniform airflow in narrow ducts.

529

530 **Table 7** Relative uncertainty calculation for the evaporative cooling modes

	<b>Inlet Air Velocity</b>	<b>Inlet Air Temp</b>	<b>Supply air DB Temp</b>	<b>Supply air WB Temp</b>	<b>Effectiveness</b>	<b>Effectiveness relative uncertainty</b>	<b>Cooling capacity</b>	<b>Cooling capacity relative uncertainty</b>
	(m/s)	(°C)	(°C)	(°C)	(%)	(%)	(W)	(%)
<b>DEC</b>	2.85	40	27.1	25.3	0.87	3.23	339.57	10.76
<b>IEC</b>	1.65	40.5	30.3	25.5	0.67	3.10	155.4	18.30
<b>DPEC</b>	1.85	41.8	31.5	25.5	0.67	3.04	174.4	16.34

531

#### 532 **4. Research limitations**

533

534 This work used experimentation to investigate the use of synthetic grass fibres as wet media in  
 535 evaporative coolers. The experimental results show overall the performance of this type of media  
 536 material is consistent and be used as a springboard for further research. One area is to consider  
 537 theoretical analysis and heat transfer optimisation of the synthetic grass fibre structure, backing  
 538 plate thickness and wet and dry channels separation gap. Equally, the uncertainty analysis  
 539 revealed that the measured cooling capacity accuracy could be improved by using more accurate



540 anemometer in measuring the airflow velocity. Finally, the energy consumption of auxiliary  
541 equipment such as fans and water circuiting pump could be considered, and the overall coefficient  
542 performance of the cooler be used as an additional performance index.

## 543 **5. Conclusions**

544

545 This research seeks to advance the design of evaporative cooling technology by investigating  
546 experimentally the performance of novel wet media material in the form of synthetic grass mats.  
547 A purpose laboratory test rig was built to test a synthetic grass fibre module in three modes of  
548 operation: DEC, IDE and DPEC. The effectiveness and cooling capacity the three arrangements  
549 were evaluated under controlled conditions of temperature, humidity, and airflow rate. The  
550 experimental results demonstrated consistency when compared to published work. This work  
551 yielded several key insights that can be summarized as follows:

- 552 • The synthetic grass fibres present a viable wet media material alternative for evaporative  
553 cooling systems that can enhance service life with maintenance.
- 554 • The three modes of operation of evaporative cooling achieved effectiveness ranging from  
555 0.67 to 0.87. Similarly, the measured maximum temperature drop in the coolers ranges  
556 from 10.1° C to 12.9° C.
- 557 • The correlation between decreasing supply air temperature as ambient inlet air  
558 temperature increases demonstrates the principle of evaporative cooling as an  
559 appropriate technology for hot and dry climates.
- 560 • The evaporative cooling systems also achieved high cooling capacities ranging from 155.4  
561 to 339.57 W. However, the system cooling capacity is reduced as air relative humidity  
562 increases, which suggest that local climatic conditions are a critical parameter for the  
563 performance of evaporative cooling systems.
- 564 • The experimental work showed that the Direct Evaporative Cooling (DEC) mode achieved  
565 higher performance. For instance, the temperature drop was nearly 20% greater than  
566 Indirect Evaporative Cooling (IEC) mode, albeit at the expense of increasing the air  
567 moisture content.

## 568 **Acknowledgements**

569

570 This research has been funded by Scientific Research Deanship at University of Ha'il - Saudi  
571 Arabia through project number -RG-23 018-

572

573

574

575 **References**

576

- 577 1. Lamsal, P., S.B. Bajracharya, and H.B. Rijal, *A Review on Adaptive Thermal Comfort*  
578 *of Office Building for Energy-Saving Building Design*. *Energies*, 2023. **16**(3): p. 1524.
- 579 2. Lamb, W.F., et al., *A review of trends and drivers of greenhouse gas emissions by*  
580 *sector from 1990 to 2018*. *Environmental research letters*, 2021. **16**(7): p. 073005.
- 581 3. Dreyfus, G., et al., *Assessment of climate and development benefits of efficient and*  
582 *climate-friendly cooling*. *Climate & Clean Air Coalition and Institute for Governance &*  
583 *Sustainable Development*, 2020.
- 584 4. Khosla, R., et al., *Sustainable Cooling in a Warming World: Technologies, Cultures,*  
585 *and Circularity*. *Annual Review of Environment and Resources*, 2022. **47**: p. 449-  
586 478.
- 587 5. Mesloub, A., et al., *Assessment of the overall energy performance of an SPD smart*  
588 *window in a hot desert climate*. *Energy*, 2022. **252**: p. 124073.
- 589 6. Al-Shamkhee, D., et al., *Passive cooling techniques for ventilation: an updated*  
590 *review*. *Renewable Energy and Environmental Sustainability*, 2022. **7**: p. 23.
- 591 7. Amer, O., R. Boukhanouf, and H. Ibrahim, *A review of evaporative cooling*  
592 *technologies*. *International journal of environmental science and development*, 2015.  
593 **6**(2): p. 111.
- 594 8. Duan, Z., et al., *Dynamic simulation of a hybrid dew point evaporative cooler and*  
595 *vapour compression refrigerated system for a building using EnergyPlus*. *Journal of*  
596 *Building Engineering*, 2019. **21**: p. 287-301.
- 597 9. Okafor, V., et al., *Energy saving potential, environmental and economic importance*  
598 *of evaporative cooling system: A review*. *European Journal of Advances in*  
599 *Engineering and Technology*, 2019. **6**(3): p. 34-45.
- 600 10. Cuce, P.M. and S. Riffat, *A state of the art review of evaporative cooling systems for*  
601 *building applications*. *Renewable and Sustainable Energy Reviews*, 2016. **54**: p.  
602 1240-1249.
- 603 11. Yang, Y., G. Cui, and C.Q. Lan, *Developments in evaporative cooling and enhanced*  
604 *evaporative cooling-A review*. *Renewable and Sustainable Energy Reviews*, 2019.  
605 **113**: p. 109230.
- 606 12. Xuan, Y., et al., *Research and application of evaporative cooling in China: A review*  
607 *(I)—Research*. *Renewable and Sustainable Energy Reviews*, 2012. **16**(5): p. 3535-  
608 3546.
- 609 13. Xuan, Y., et al., *Research and applications of evaporative cooling in China: A review*  
610 *(II)—Systems and equipment*. *Renewable and Sustainable Energy Reviews*, 2012.  
611 **16**(5): p. 3523-3534.
- 612 14. Kumar, S., et al., *Comparative performance analysis of a static & dynamic*  
613 *evaporative cooling pads for varied climatic conditions*. *Energy*, 2021. **233**: p.  
614 121136.
- 615 15. da Veiga, A.P., S. Güths, and A.K. da Silva, *Evaporative cooling in building roofs:*  
616 *Theoretical modeling and experimental validation (Part-1)*. *Solar Energy*, 2020. **207**:  
617 p. 1122-1131.
- 618 16. Kowalski, P. and D. Kwiecień, *Evaluation of simple evaporative cooling systems in an*  
619 *industrial building in Poland*. *Journal of Building Engineering*, 2020. **32**: p. 101555.
- 620 17. Lapis, R., et al., *Optimized design of low-rise commercial buildings under various*  
621 *climates—Energy performance and passive cooling strategies*. *Building and*  
622 *Environment*, 2018. **132**: p. 83-95.
- 623 18. Alshenaifi, M.A., et al., *Numerical Analysis of Building Cooling Using New Passive*  
624 *Downdraught Evaporative Tower Configuration in an Arid Climate*. *Mathematics*,  
625 2022. **10**(19): p. 3616.
- 626 19. He, W., et al., *Research of evaporative cooling experiment in summer of residential*  
627 *buildings in Xi'an*. *Energy Procedia*, 2018. **152**: p. 928-934.

- 628 20. Dhamneya, A.K., S. Rajput, and A. Singh, *Theoretical performance analysis of*  
629 *window air conditioner combined with evaporative cooling for better indoor thermal*  
630 *comfort and energy saving*. Journal of Building Engineering, 2018. **17**: p. 52-64.
- 631 21. Boukhanouf, R., et al., *Design and performance analysis of a regenerative*  
632 *evaporative cooler for cooling of buildings in arid climates*. Building and Environment,  
633 2018. **142**: p. 1-10.
- 634 22. Moosavi, L., M. Zandi, and M. Bidi, *Experimental study on the cooling performance of*  
635 *solar-assisted natural ventilation in a large building in a warm and humid climate*.  
636 Journal of Building Engineering, 2018. **19**: p. 228-241.
- 637 23. Leroux, G., et al., *Innovative low-energy evaporative cooling system for buildings:*  
638 *study of the porous evaporator wall*. Journal of Building Performance Simulation,  
639 2019. **12**(2): p. 208-223.
- 640 24. Zhang, L., et al., *Impact of climatic factors on evaporative cooling of porous building*  
641 *materials*. Energy and Buildings, 2018. **173**: p. 601-612.
- 642 25. Duan, Z., et al., *Indirect evaporative cooling: Past, present and future potentials*.  
643 Renewable and sustainable energy reviews, 2012. **16**(9): p. 6823-6850.
- 644 26. Ali, M., et al., *Performance enhancement of a cross flow dew point indirect*  
645 *evaporative cooler with circular finned channel geometry*. Journal of Building  
646 Engineering, 2021. **35**: p. 101980.
- 647 27. Lin, J., et al., *The counter-flow dew point evaporative cooler: Analyzing its transient*  
648 *and steady-state behavior*. Applied Thermal Engineering, 2018. **143**: p. 34-47.
- 649 28. Al-Mogbel, A., et al., *Experimental investigations of evaporative cooling system for*  
650 *buildings under hot and dry environmental conditions*. Heat Transfer Research, 2020.  
651 **51**(9).
- 652 29. Zhao, X., S. Liu, and S.B. Riffat, *Comparative study of heat and mass exchanging*  
653 *materials for indirect evaporative cooling systems*. Building and Environment, 2008.  
654 **43**(11): p. 1902-1911.
- 655 30. Amer, O., R. Boukhanouf, and H.G. Ibrahim, *A review of evaporative cooling*  
656 *technologies*. International journal of environmental science and development, 2015.  
657 **6**(2): p. 111.
- 658 31. Jastifer, J.R., et al., *Synthetic turf: history, design, maintenance, and athlete safety*.  
659 Sports health, 2019. **11**(1): p. 84-90.
- 660 32. Serensits, T.J., A.S. McNitt, and J.C. Sorochan, *Synthetic turf*. Turfgrass: Biology,  
661 use, and management, 2013. **56**: p. 179-217.
- 662 33. Schoukens, G., *Developments in textile sports surfaces*, in *Advances in carpet*  
663 *Manufacture*. 2009, Elsevier. p. 101-133.
- 664 34. Almazroui, M., et al., *Regional and seasonal variation of climate extremes over Saudi*  
665 *Arabia: observed evidence for the period 1978–2021*. Arabian Journal of  
666 Geosciences, 2022. **15**(20): p. 1605.
- 667 35. Phillip, T. and B. Lau. *PASSIVE DOWNDRAUGHT EVAPORATIVE COOLING : The*  
668 *Applicability for residential space cooling in Riyadh , Saudi Arabia*. 2013.
- 669 36. Musa, M.a., *Novel evaporative cooling systems for building applications*. PhD diss.,  
670 University of Nottingham, 2009.
- 671 37. Ibrahim, E., L. Shao, and S.B. Riffat, *Performance of porous ceramic evaporators for*  
672 *building cooling application*. Energy and Buildings, 2003. **35**(9): p. 941-949.
- 673 38. Ford, B., R. Schiano-Phan, and E. Francis, *The architecture and engineering of*  
674 *downdraught cooling: a design source book*. 2010: PHDC press.
- 675 39. Kanzari, M., R. Boukhanouf, and H.G. Ibrahim, *Mathematical modeling of a sub-wet*  
676 *bulb temperature evaporative cooling using porous ceramic materials*. International  
677 Journal of Industrial and Manufacturing Engineering, 2013. **7**(12): p. 900-906.
- 678 [40] Lv, J., Xu, T., Liu,H., Qin,J., Study on the performance of a unit dew-point evaporative cooler with  
679 fibrous membrane and its application in typical regions, Case Studies in Thermal Engineering,  
680 2021. 24

681  
682